Coherent Imaging with Hard X-rays

Anatoly SNIGIREV
ESRF, Grenoble, France

- Why do we need coherent hard X-rays?
  - absorption vs phase contrast
  - holography/phase contrast imaging, present status
  - microoptics & scanning microscope
- Requirements to the optics
- What can we do with XFEL?

Third generation SR sources

High flux	10^{14} ph/s/0.1%/mm^2
High collimation (low divergence)	~ 10 μrad
Small source size (coherence)	25 μm (FWHM)

pinholes
capillaries
waveguides

BFO
FZP
refractive lenses

Optics more ellegant
small aperture
high resolution

High resolution detectors

High energy X-ray Microscopy:

imaging **diffraction**
holography **fluorescence**
tomography **spectroscopy**

High Energy X-ray Microscopy

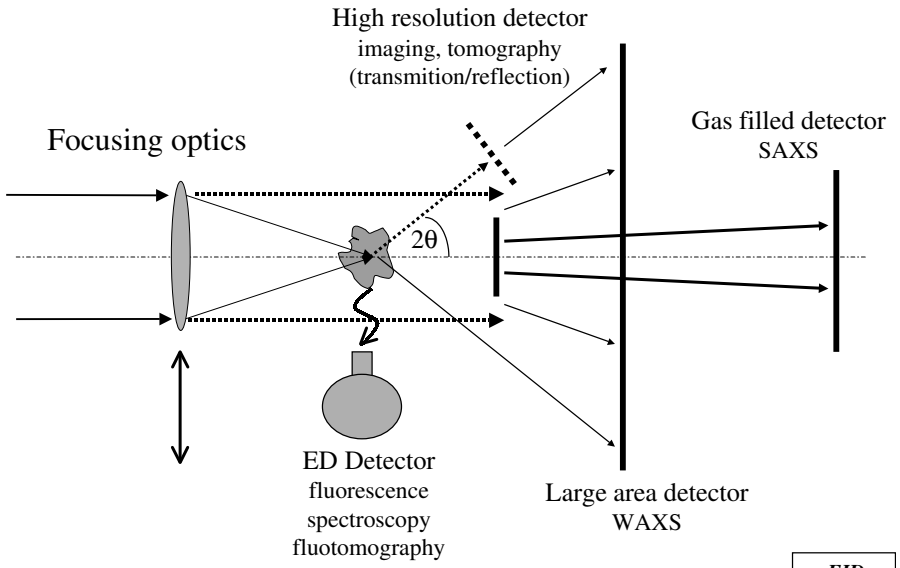

applications

- Biomedicine
  (prosthesis, tumor spheroids, single cells, fiber diffraction)
- Material science
  (microelectronics, Cu-wiring, single grains, paper)
- Geology
  (microfluids, rocks samples, clay minerals etc.)
- Astrophysics
  (micro-meteorites)
- Environmental science
  (dust U-particles, ash-fly particles, sea shells etc.)
- Archeology
  (roman glas)

X-Ray Imaging

- Full-field microscopy with incoherent illumination

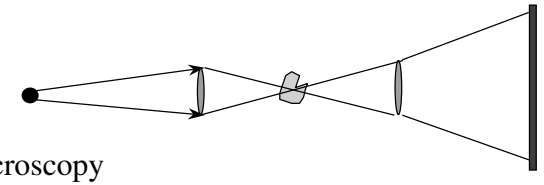

- Scanning microscopy

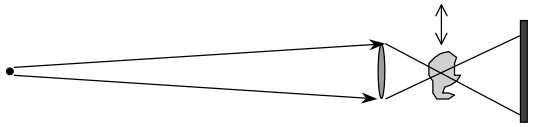

- Full-field imaging with coherent illumination

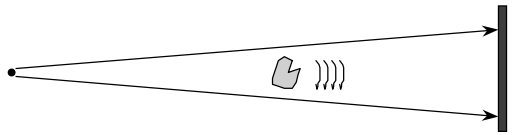

XFEL vs Undulator

ID22, high-β undulator

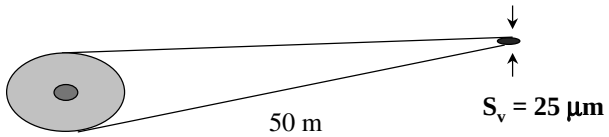

1mm* 1mm

Flux ~ 10^{13} ph/s/Si-111

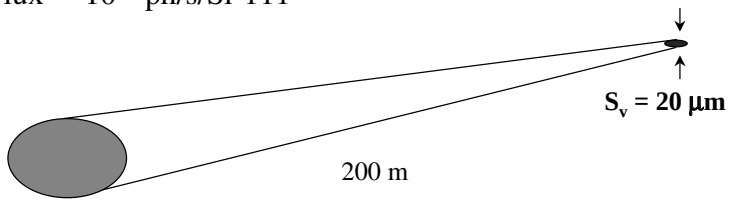

1 mm^2 *Fully coherent!*

Flux gain x 10^5 - 10^7

Properties of ESRF X-ray sources

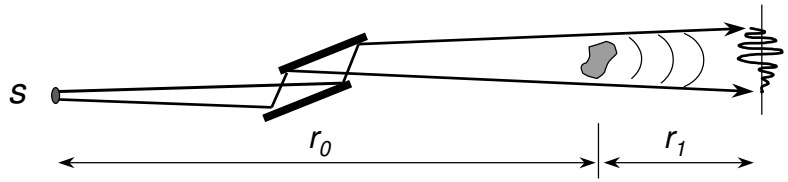

- high photon flux
  - 10^{13} ph/sec/mm^2/Si-bw (high-β-sections)
- highly coherent beam

  small source size s ~ 25 μm → spatial coherence

  large source distance r_0 ~ 50 m → $r_0\lambda / s$ ~ **200 μm** (λ =1Å)

  ↓

  angular source size: ~ 0.5 μrad

  Si-111 Δθ ~ 20 μrad (λ =1Å, E = 12.4 keV)

  Si-555 Δθ ~ 0.5 μrad (λ =1Å, E = 30 keV)

Coherence Characterisation by Fresnel Diffraction / Slits

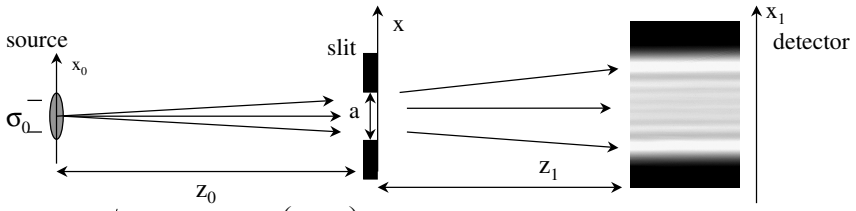

$$I(x_1) = 1 + \frac{4}{\pi}\left(\frac{4\lambda z_0 z_1}{z a^2}\right)^{1/2} \cos\left(\frac{\pi z a^2}{4\pi z_0 z_1} - \frac{3\pi}{4}\right) \exp\left(-\frac{a^2}{4\sigma_{mc}^2}\right) \cos\left(\frac{\pi a}{\lambda z_1} x_1\right)$$

$$V(x_1) = \frac{I(x_1)_{\max} - I(x_1)_{\min}}{I(x_1)_{\max} + I(x_1)_{\min}}$$

$$V = V_0 \exp\left(-\frac{a^2}{4\sigma_{mc}^2}\right), \quad \sigma_{mc} = \frac{2\lambda z_0}{\pi \sigma_0} \quad \Rightarrow \quad \sigma_0 = \frac{4\lambda z_0}{\pi a} \ln^{1/2}\left(\frac{V_0}{V}\right)$$

$$V_0 = \frac{4}{\pi}\left(\frac{4\lambda z_0 z_1}{z a^2}\right)^{1/2} \left|\cos\left(\frac{\pi z a^2}{4\pi z_0 z_1} - \frac{3\pi}{4}\right)\right|$$

$$a \geq 3\left(\frac{2\lambda z_0 z_1}{z}\right)^{1/2}, \quad x_1 = \frac{az}{10 z_0}$$

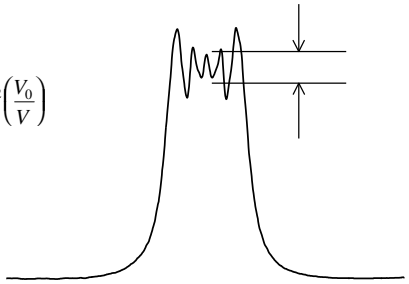

Polished Be : 0.1μm
2 000 kFF

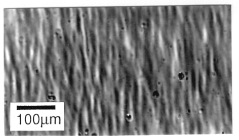

Be windows

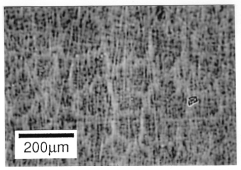

Green paper

Polished filters (Si)
FE- diamond
(no graphite)

Multilayers

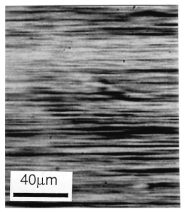

Multilayers

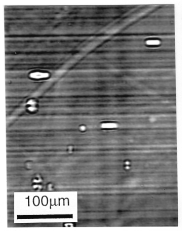

Mirrors

Super Polished mirrors
<1Å, <1μrad
horiz. deflection

Micro-scratches
Chemical etching

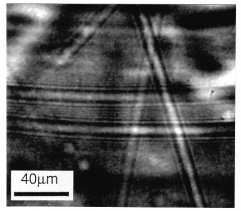

Crystals

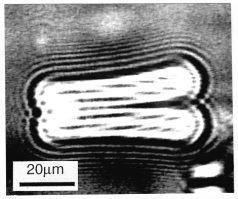

Dust particles

Cleaning !?

Phase contrast imaging and tomography

Phase-Contrast Imaging

$E(\vec{r}) = A_0 e^{-i\vec{k}\vec{r}}$

X-ray beam

object
n=1-δ+iβ

absorption coefficient β

Absorption
$A(z) = A_0 e^{-\beta z/2}$

decrement of refractive index δ

Phase-Shift
$A(z) = A_0 e^{i\delta z}$

5 keV < *E* < 60 keV
2.5 Å > λ > 0.1 Å

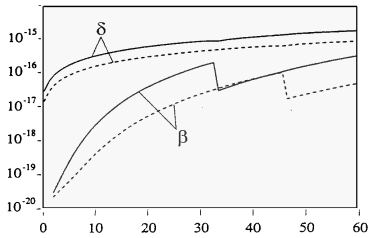

β and δ plotted versus atomic number *Z*
for 1 Å (solid line) and 0.5 Å (dotted line).
(From Momose, Med Phys. 1995)

For hard X-rays δ is 1000x larger than β

\+ detecting the phase of the object wave is more sensitive

\- only intensity, not amplitude and phase of wave can be measured

Bonse-Hart Interferometer

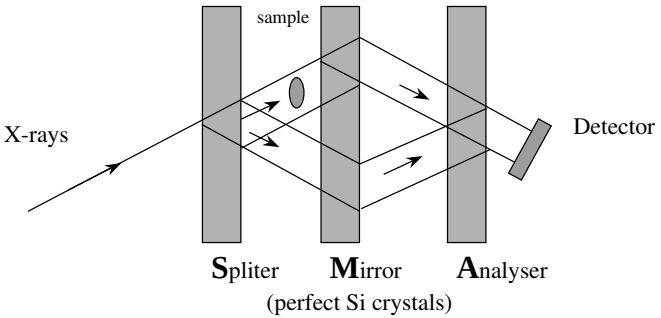

Bonse & Hart, 1965

Momose, 1995 **Phase contrast imaging and tomography**

E=10-20keV
resolution ~ 10-20µm

Coherent Image Formation

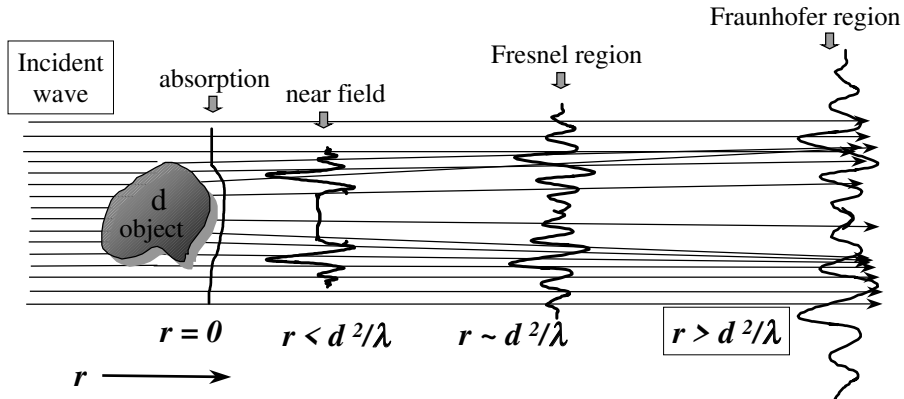

	d	*r ~ d ²/λ*
soft X-rays λ > 10 A	1 10 100	1 mm 0.1 m 10 m
hard X-rays λ < 1 A	1 10 100	10 mm 1 m 100 m

XFEL!

Coherent Imaging of Non-absorbing Samples

Boron fiber
(100µm diameter)
E = 16 keV

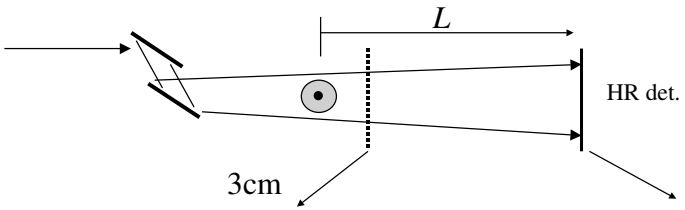

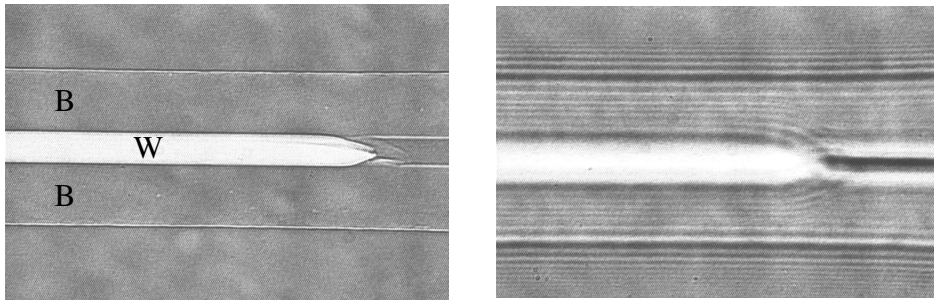

Lens-Coupled CCD Detector

Resolution ~ 0.7µm!
at 20 keV

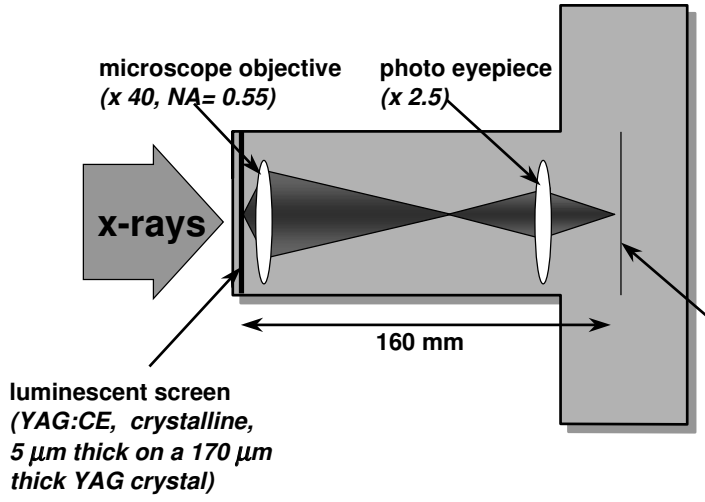

High Energy X-ray Phase Contrast Tomography with µm-Resolution

C. Raven, I. Snigireva, A. Snigirev, ESRF

E = 18 keV

Daddylonglegs knee

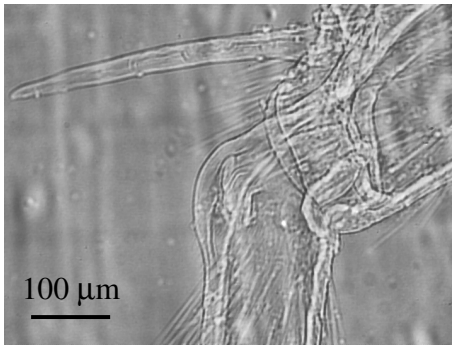

Phase contrast image

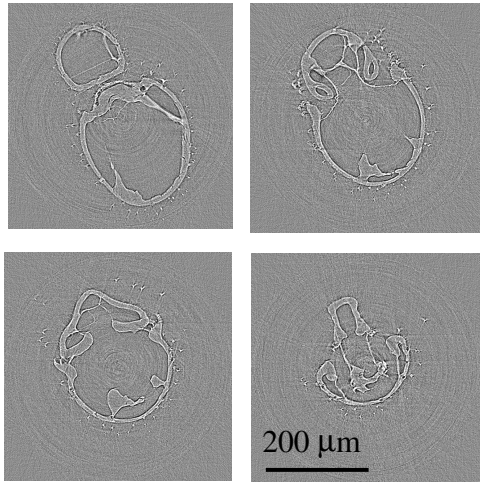

Cross sections through an insect's knee

µ-FID$_{22}$

Imaging of the head of a weevil

G. Troester and T. Hoernschemeyer, Inst. für Zoologie und Anthropologie, Göttingen, Germany
T. Weitkamp, A. Snigirev, ESRF, Grenoble, France

Beetle with a beaklike rostrum

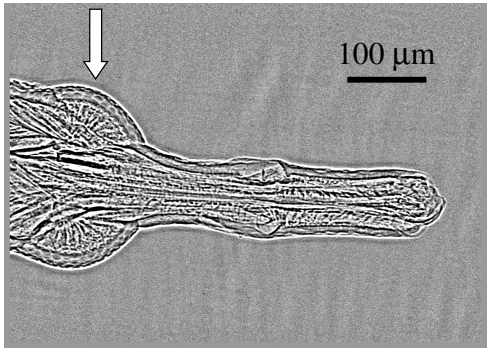

Phase contrast projection image

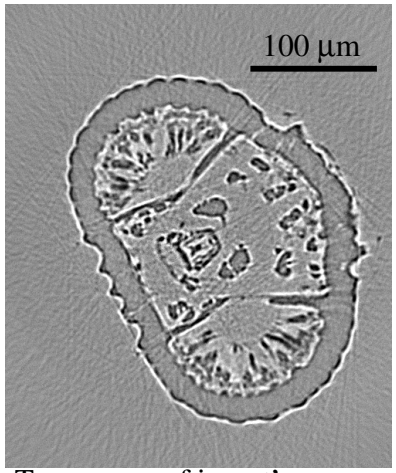

Tomogram of insect's eyes
1250 projections

µ-FID$_{22}$

Uranium Dust Particle

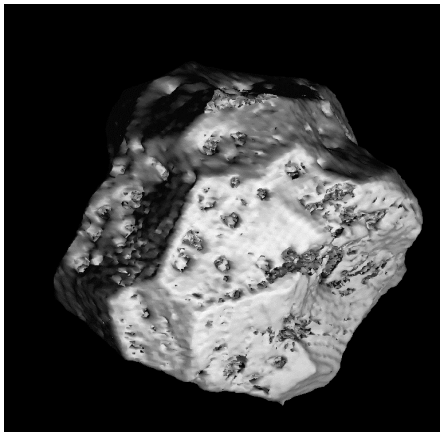

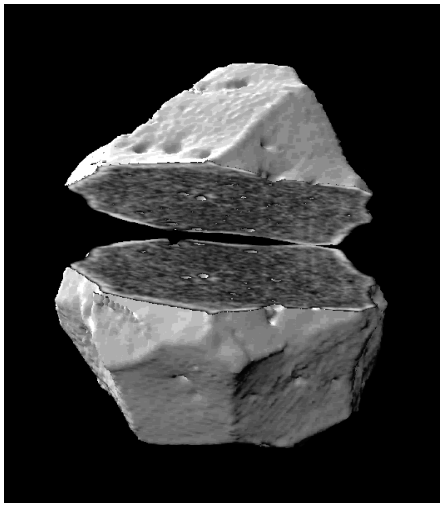

E = 17.2 keV
200 projections, 2 hrs total time,
resolution ~ 0.7µm

µ-FID$_{22}$

Phase contrast and XANES microtomography of Uranium particles

250 projections
<1hr for dual energy
resolution ~1µm

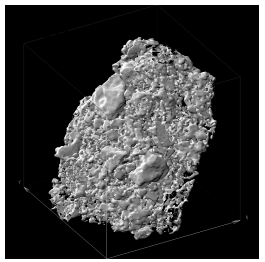

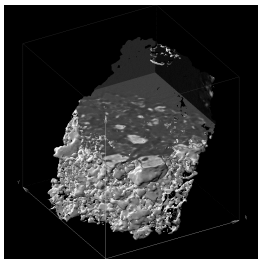

17.2 keV **17.1 keV**

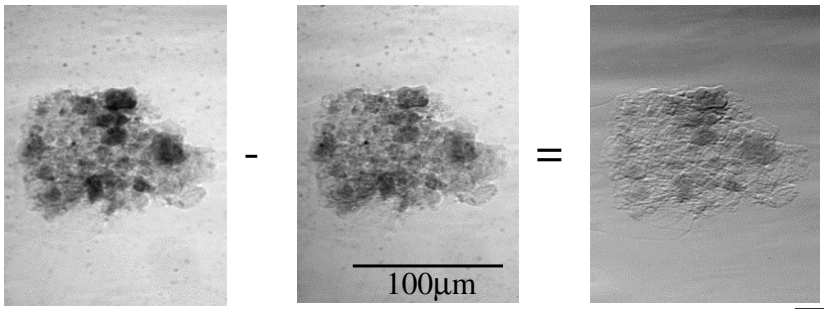

µ-FID$_{22}$

Coherent X-ray imaging of microelectronics structures

N. Awaji (Fujitsu), M. Drakopoulos, I. Snigireva, A. Snigirev (ESRF)

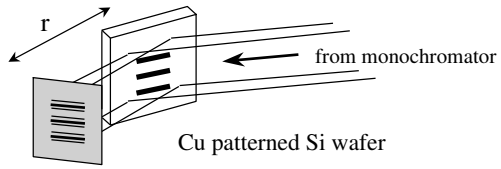

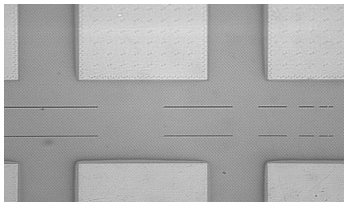

E = 12keV
reflection-400

Cu lines
2.5 - 200 μm length
0.3 μm thickness

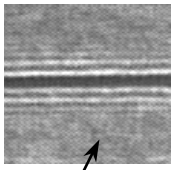

r = 3 cm

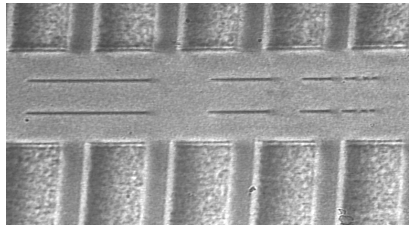

100 μm

r = 12 cm

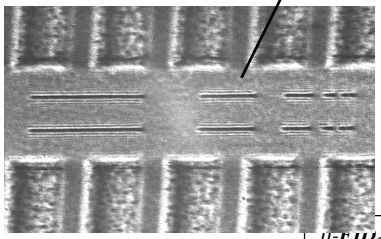

Time-resolved imaging

An extraordinary CCD camera

The ***FReLoN 2000*** (Fast Readout Low Noise) CCD camera is an ESRF inhouse development. Technical data:

- Chip size: 2048 x 2048 pixels
- Pixel size: 14 um
- Dynamic range: 14-bit
- Readout noise: 1 electron / s
- Readout time: 0.2 s for a full frame

These outstanding characteristics allow the use of FReLoN-based imaging systems for purposes where ***speed*** and/or ***intensity*** are critical issues, notably microscopy and high-speed imaging. At ID22, the FReLoN is used with microscope optics specially designed for the needs of this beamline .

Example:

Time-resolved study of dendrite growth in an alloy solidification process

Sn-10wt%Pb

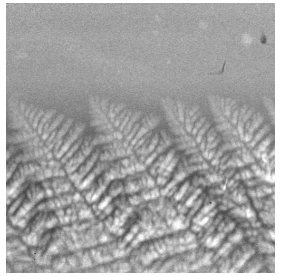

- Columnar dendritic grows of Sn crystals
- Exposure time: 0.1 s
- Repeat rate: 2 Hz

Collaboration with R. Mathiesen, NTNU Trondheim, Norway

Present status of 1Å imaging

- Absorbtion radiography, tomography > 5 μm
- Phase contrast tomography (LLL-interferometer)
  - 20μm (Bonse, Momose)
- Phase contrast imaging
  - 0.7 μm without x-ray optics
  - 0.3μm with x-ray optics
- Phase contrast tomography
  - 1μm
- Diffraction topography
  - 0.7μm

Next steps in phase contrast imaging.

- Time resolved imaging
- "Pink" beam imaging
- X-ray microscopy with lenses (FZP and CRL)
- Holography / Refractive index reconstruction

"Pink-beam" imaging

Idea: Use of one undulator harmonic instead of a conventionally monochromatized beam

Application fields:
- X-ray microscopy
- Time-resolved imaging

Monochromatic vs. pink beam: Interference fringes from a Boron fiber with tungsten core

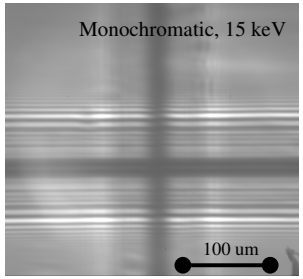

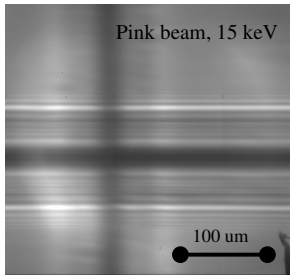

Phase-contrast image of a spider leg

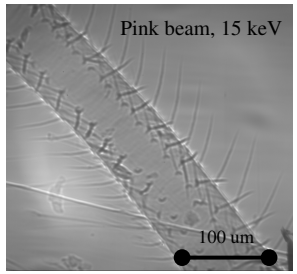

In-line Holography

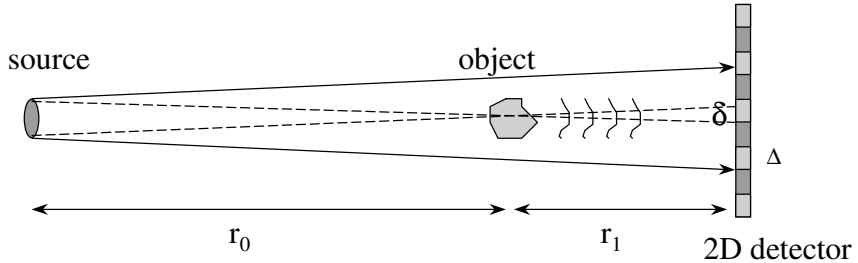

source size	s
wavelength	λ
source-to-object distance	r_0
object-to-detector distance	r_1
object size	d
detector resolution	Δ

spatial coherence

$\lambda r_0/s$ **for ESRF 100μm at 50m**

holographic resolution

$\delta = s\, r_1/r_0$

for an XFEL spatial coherence = *beam size* ~ $s + r_0$ * *divergence* = **150μm at 50m**

Why do we need a coherent beam for Microoptics?

Transverse coherence ~ Aperture of the optics
- Diffraction limited focusing at subμm level
- Coherent secondary source - coherence inhancement

Aperture (acceptance) of the diffraction optics is about 100 -500 μm with resolution ~ 0.1μm

Transverse coherence at the ESRF is about 200 μm

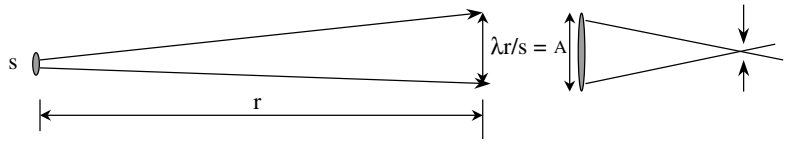

Micro-fluorescence/spectroscopy and Micro-diffraction

Fluorescence imaging

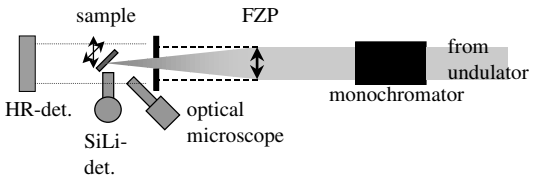

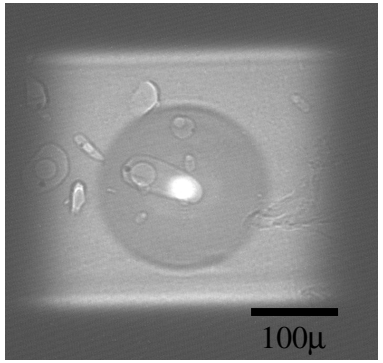

Fresnel zone plate
Focal spot size: 0.5 µm (V) x 6 µm (H)
Flux: 10^{10} photons/s, 12.5 keV

Micro analysis(Cu, Zn, As) of geological samples:
(from gold-quartz vein at Brusson, Italian Alps)

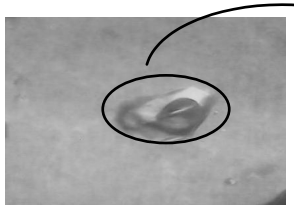

Arsenic distribution in a fluid inclusion

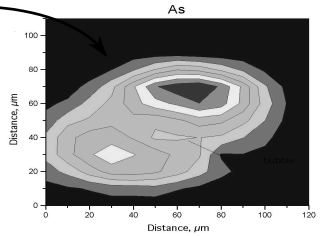

µ-FID$_{22}$

Influence of the heterogeneously distributed stored energy on recrystallization processes in steel

O. Castelnau, T. Chauveau (LPMTM-CNRS, Paris)
T. Ungar (University, Budapest)

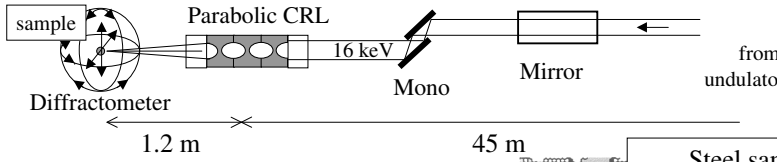

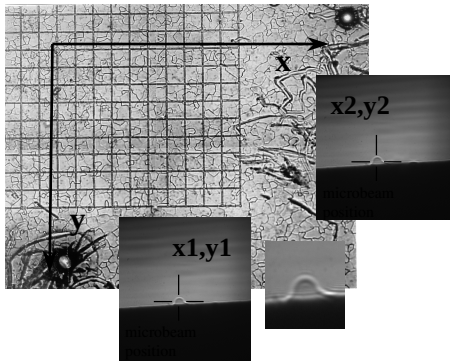

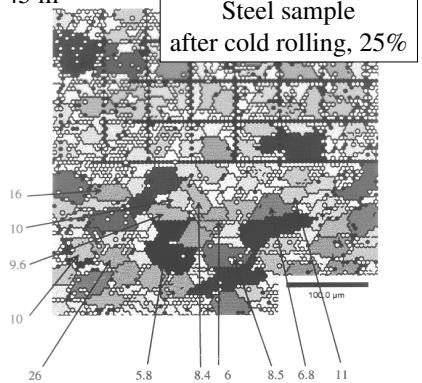

µ-FID$_{22}$

X-ray Microoptics

µ-FID$_{22}$

Focusing Optics for Hard X-rays
Energy: (2) 6 - 30 (100) keV

	Kinematical Focusing Bent mirror or crystal			Capillaries	Waveguides	Fresnel optics	Bragg-Fresnel Optics		Refractive optics
				Kreger 1948	Feng et al 1993	Baez 1952	Aristov et al, 1986		Snigirev et al, 1996
	mirror	multilayer	crystal		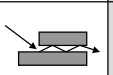	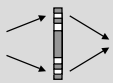			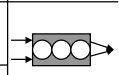
	Kirkpatrick Baez, 1948	Underwood Barbee, 1986	Johann, Johansson, 1931-1933				ML	crystal	
accept	0.2 mm	0.2 mm	1 mm	0.1 mm	~10 µm	0.5 mm	~1 mm		~1 mm
gain	10^4	10^4	10^4	10^2	<10	10^4	10^4		10^2 -10^3
E	<20keV	<80keV	<100keV	<20keV	<20keV	<20keV	<100keV		<100keV
$\Delta E/E$	w. b.	10^{-2}	10^{-4} -10^{-6}	10^{-3}	10^{-3}	10^{-3}	10^{-2}	10^{-4} -10^{-6}	10^{-2}
flux(ph/s)	10^8 (9keV)	10^{10} (12keV)	10^9 (90keV)	10^9 (8keV)	10^9 (10keV)	10^9 (9keV)	10^9 (10keV)	10^9 (10keV)	10^9 (20keV)
resolution	**0.7 µm** Iida 1996	**0.7 µm** Thompson 1996	**1.2 µm** Linnert 1997	**0.05 µm** Bielderbeck 1994	**0.15 µm** Lagomarsino 1996	**0.15 µm** Yun1998 ~20nm<1keV	**0.9 µm** Erko 1995	**0.5 µm** Snigirev 1996	**0.3 µm** Schroer 1999

µ-FID$_{22}$

Fresnel Zone Plate

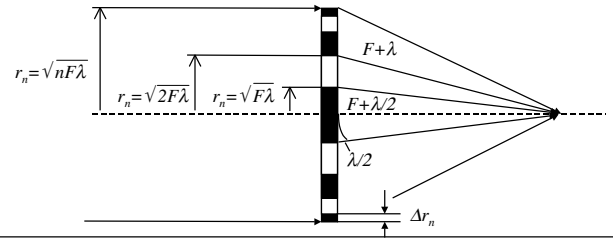

Amplitude FZP
alternate zones - opaque

efficiency ~ 10%

Phase FZP
alternate zones - phase shifting

efficiency ~ 40%

$t = \Delta r_n$

Kinoform FZP
(sawtooth profile)

efficiency ~ 70 - 100%

"State of the art" APS/Wisconsin- CXRL/Rome-IESS

Δr_n ~ 0.1μm	res. ~	**0.15 μm**
aspect ratio $\Delta r_n / t$ ~ 10	energy ~	**20 (30) keV**
4-6 levels for sawtooth ZP	eff. ~	**60 %**

!

μ-FID$_{22}$

FZP

FZP 1*

A = 200 μm
r_1 = 7.8 μm
Δr_n = 0.3 μm
t_{Au} = 1.15 μm
F = 40 cm at 8 keV
F = 60 cm at 12 keV
flux 10^{10} photons/sec

* Provided by IESS, CNR, Rome, Italy

FZP 2**

A = 600 μm
r_1 = 12.45 μm
Δr_n = 0.25 μm
t_{Au} = 1. 5 μm
F = 100 cm at 8 keV
F = 150 cm at 12 keV
flux 10^{11} - 10^{12} photons/sec

** provided by APS (Argonne, USA) through a collaboration with the Centre for X-ray Lithography (U. of Wisconsin-Madison, USA) and IESS, CNR, Rome, Italy

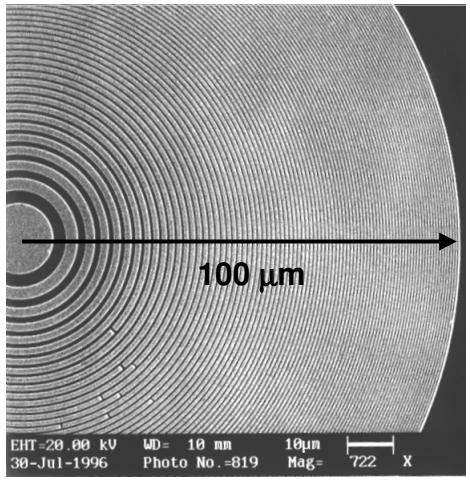

Res. ~ 0.4 - 0.5 μm

μ-FID$_{22}$

Focusing Optics for Hard X-rays
Energy: (2) 6 - 30 (100) keV

	Kinematical Focusing Bent mirror or crystal			Capillaries	Waveguides	Fresnel optics	Bragg-Fresnel Optics		Refractive optics
				Kreger 1948	Feng et al 1993	Baez 1952	Aristov et al, 1986		Snigirev et al, 1996
	mirror	multilayer	crystal						
	Kirkpatrick Baez, 1948	Underwood Barbee, 1986	Johann, Johansson, 1931-1933				ML	crystal	
accept	0.2 mm	0.2 mm	1 mm	0.1 mm	~10 μm	0.5 mm	~1 mm		~1 mm
gain	10^4	10^4	10^4	10^2	<10	10^4	10^4		10^2 -10^3
E	<20keV	<80keV	<100keV	<20keV	<20keV	<20keV	<100keV		<100keV
ΔE/E	w. b.	10^{-2}	10^{-4} -10^{-6}	10^{-3}	10^{-3}	10^{-3}	10^{-2}	10^{-4} -10^{-6}	10^{-2}
flux(ph/s)	10^8 (9keV)	10^{10} (12keV)	10^9 (90keV)	10^9 (8keV)	10^9 (10keV)	10^9 (9keV)	10^9 (10keV)	10^9 (10keV)	10^9 (20keV)
resolution	**0.7 μm** Iida 1996	**0.7 μm** Thompson 1996	**1.2 μm** Linnert 1997	**0.05 μm** Bielderbeck 1994	**0.15 μm** Lagomarsino 1996	**0.15 μm** Yun 1998	**0.9 μm** Erko 1995	**0.5 μm** Snigirev 1996	**0.3 μm** Schroer 1999

μ-FID$_{22}$

Bragg-Fresnel Optics

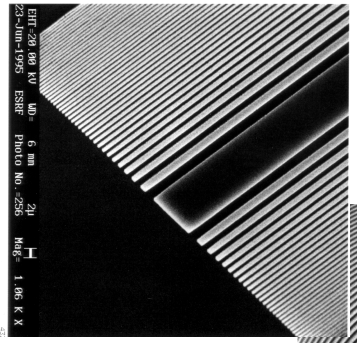

Linear BFL
Si (111)
A = 200 μm
Δr_n = 0.3 μm

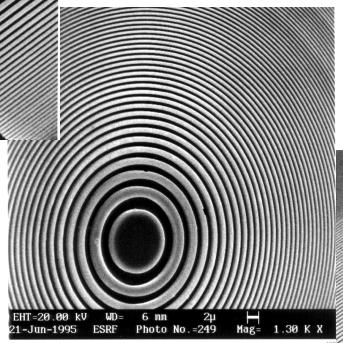

Multilayer BFL elliptical
W / Si, 56 periods
length = 18 mm
width = 136 μm
Δr_n = 0.3 μm

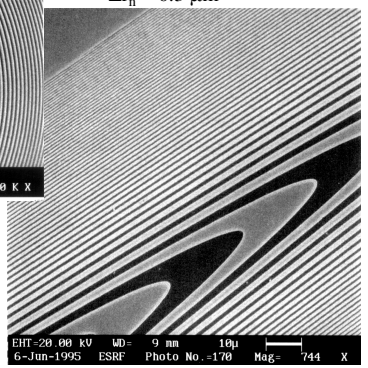

Circularar BFL
Ge (111)
A = 200 μm
Δr_n = 0.3 μm

PSI, C. David
Δr_n = 0.1 μm
aspect ratio ~ 10
aperture > 1 mm

Focusing Optics for Hard X-rays
Energy: (2) 6 - 30 (100) keV

	Kinematical Focusing Bent mirror or crystal			Capillaries	Waveguides	Fresnel optics	Bragg-Fresnel Optics		Refractive optics
				Kreger 1948	Feng et al 1993	Baez 1952	Aristov et al, 1986		Snigirev et al, 1996
	mirror	multilayer	crystal						
	Kirkpatrick Baez, 1948	Underwood Barbee, 1986	Johann, Johansson, 1931-1933				ML	crystal	
accept	0.2 mm	0.2 mm	1 mm	0.1 mm	~10 μm	0.5 mm	~1 mm		~1 mm
gain	10^4	10^4	10^4	10^2	<10	10^4	10^4		10^2 -10^3
E	<20keV	<80keV	<100keV	<20keV	<20keV	<20keV	<100keV		<100keV
ΔE/E	w. b.	10^{-2}	10^{-4} -10^{-6}	10^{-3}	10^{-3}	10^{-3}	10^{-2}	10^{-4} -10^{-6}	10^{-2}
flux(ph/s)	10^8 (9keV)	10^{10} (12keV)	10^9 (90keV)	10^9 (8keV)	10^9 (10keV)	10^9 (9keV)	10^9 (10keV)	10^9 (10keV)	10^9 (20keV)
resolution	**0.7 μm** Iida 1996	**0.7 μm** Thompson 1996	**1.2 μm** Linnert 1997	**0.05 μm** Bielderbeck 1994	**0.15 μm** Lagomarsino 1996	**0.15 μm** Yuni 1998	**0.9 μm** Erko 1995	**0.5 μm** Snigirev 1996	**0.3 μm** Schroer 1999

μ-FID22

X-rays versus Light

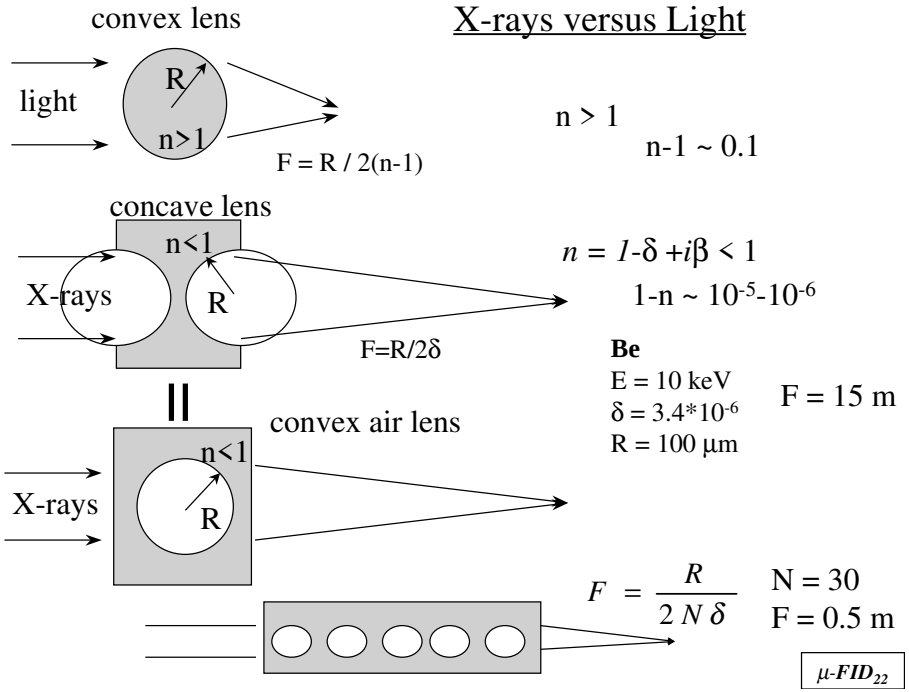

μ-FID22

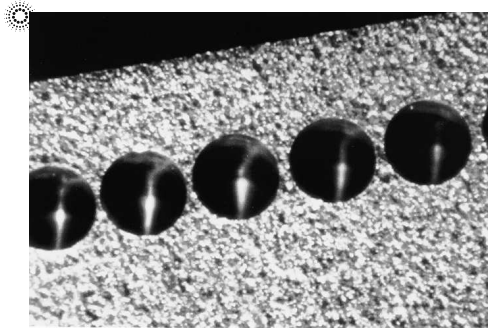

Linear Be CRL

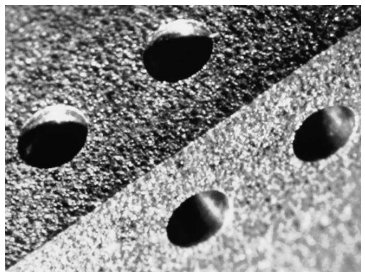

Crossed Be CRL

Cylindrical Be refractive lens

E = 9 keV
N = 69 holes
R = 250 μm
F = 1 m

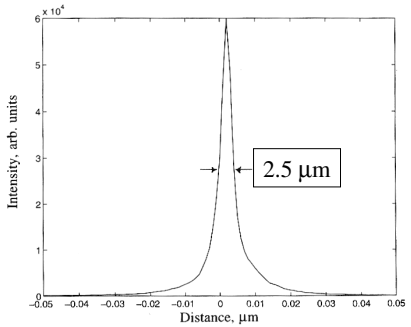

μ-FID22

(5 ESRF beamlines have FE refr. lenses)

ID 22

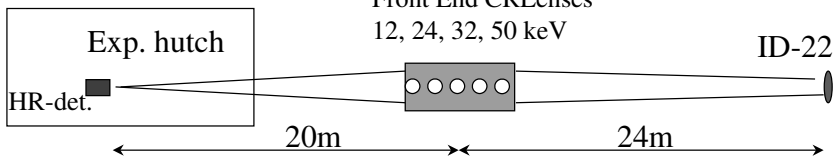

Source size $S_V * S_H = 30 * 700\ \mu m^2$
Focal Distance *11 m*

FE CRL	***12 keV***	***24 keV***	***32 keV***	***50 keV***
Material	Be	Be	Be	C
N holes	8	32	56	90
R μm	400	400	400	350
d, μm	50	50	50	50
Energy, keV	11.3	21.1	30.31	49.7
Gain	13	10	13	6
FWHM, μm	45	45	22	28
roughness, μm	6/2	12/2	12/2	20/2

μ-FID22

From cylindrical to parabolic CRL

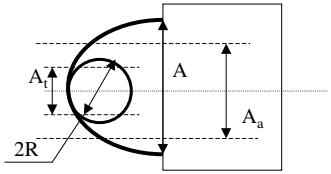

- Focusing in two directions
- Almost free of spherical aberrations
- Radius of curvature and geometrical aperture can be choosen independently
- Transmission better than for crossed cylindrical lenses
- Easier to manufacture than lenses with spherical profile

Parabolic CRL

B.Lengeler, C.Schroer, J.Tummler
RWTH, Aachen, Germany

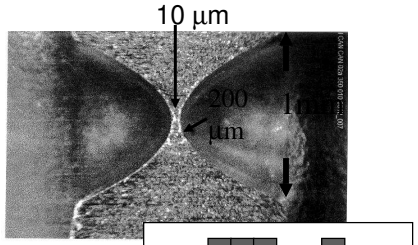

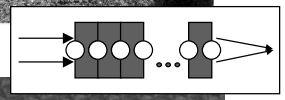

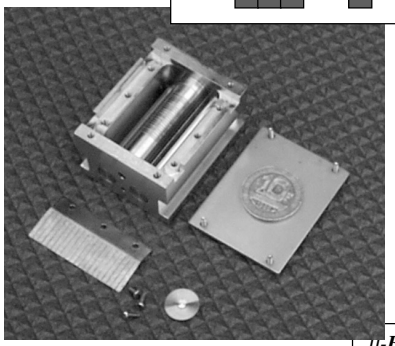

Focusing with Al parabolic CRL

December 98
E = 15 keV
N = 33 lenses
F = 1.257 m

Gain = 177

June 99 (C. Schroer)
E = 20 keV
N = 89 lenses
F = 0.6 m
flux ~ 10^{10}ph/s
res. ~ 0.6 μm

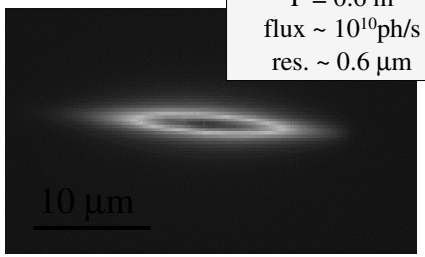

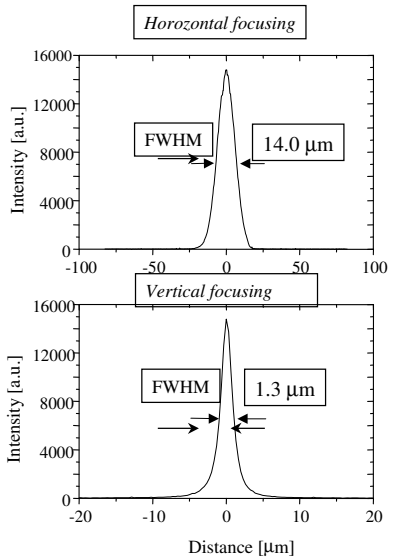

Full-field X-ray microscopy with sub-micrometer resolution

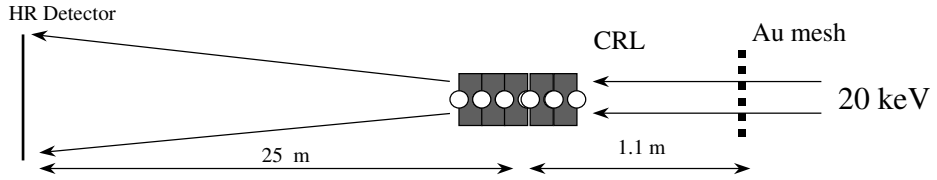

X-ray image without lens

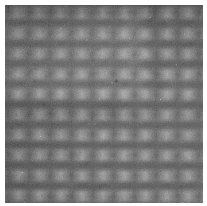

x 22

50μ

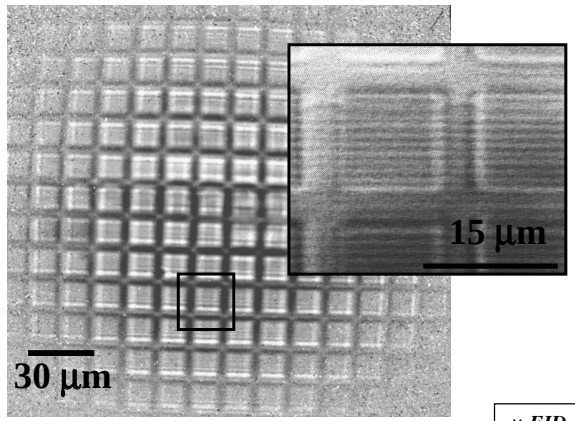

Full-field X-ray microscopy with sub-micrometer resolution

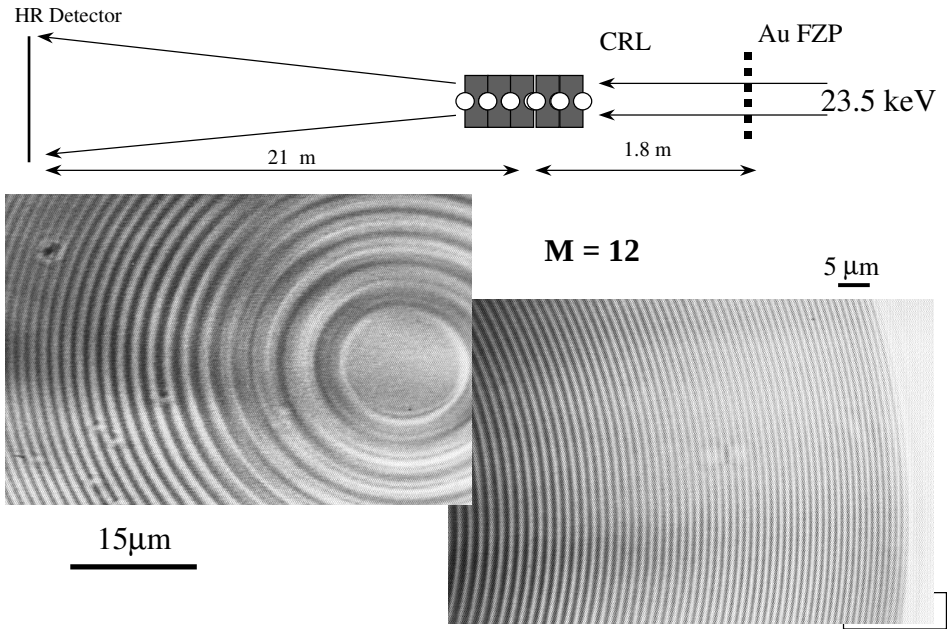

Phase Contrast Microscopy

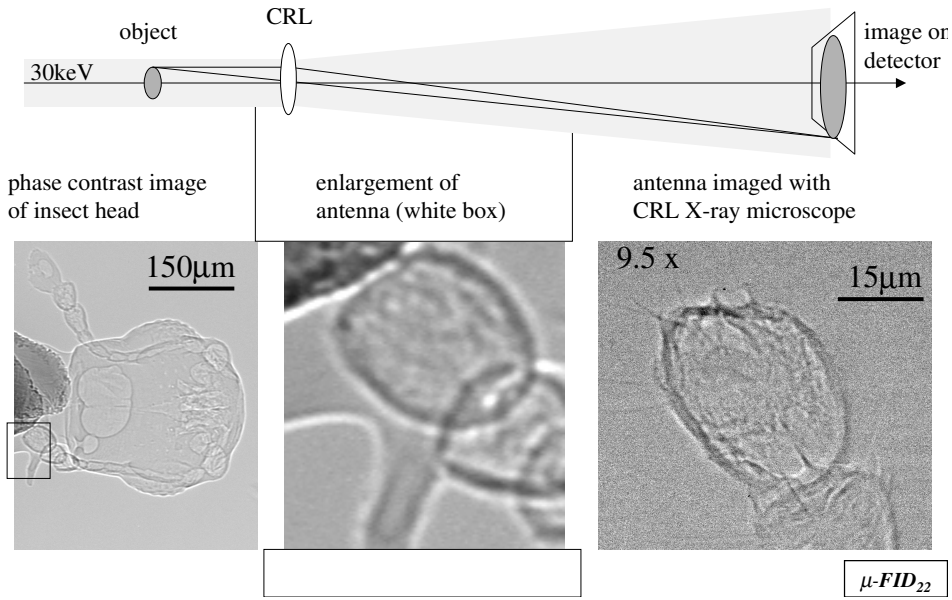

Fourier Transform Imaging

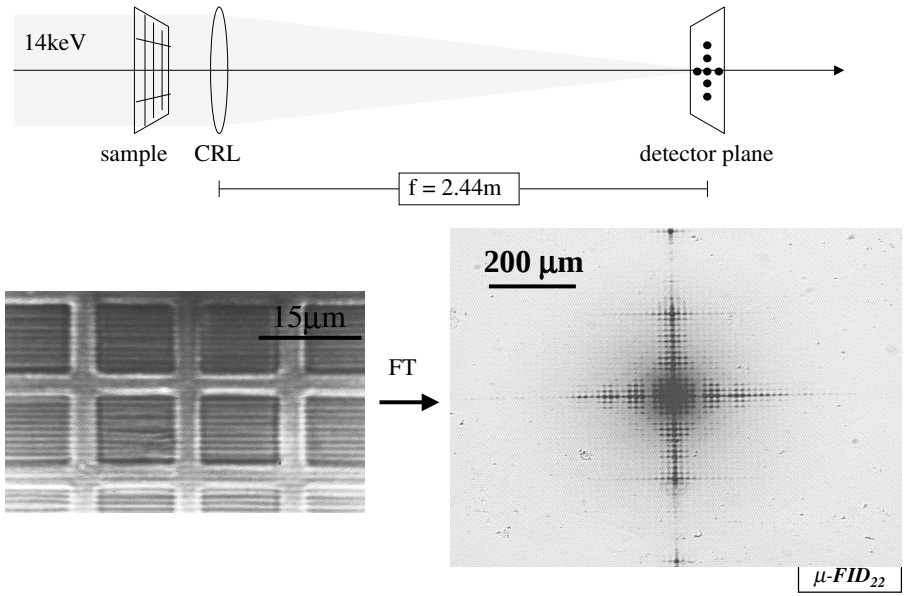

Imaging with Parabolic Refractive Lens

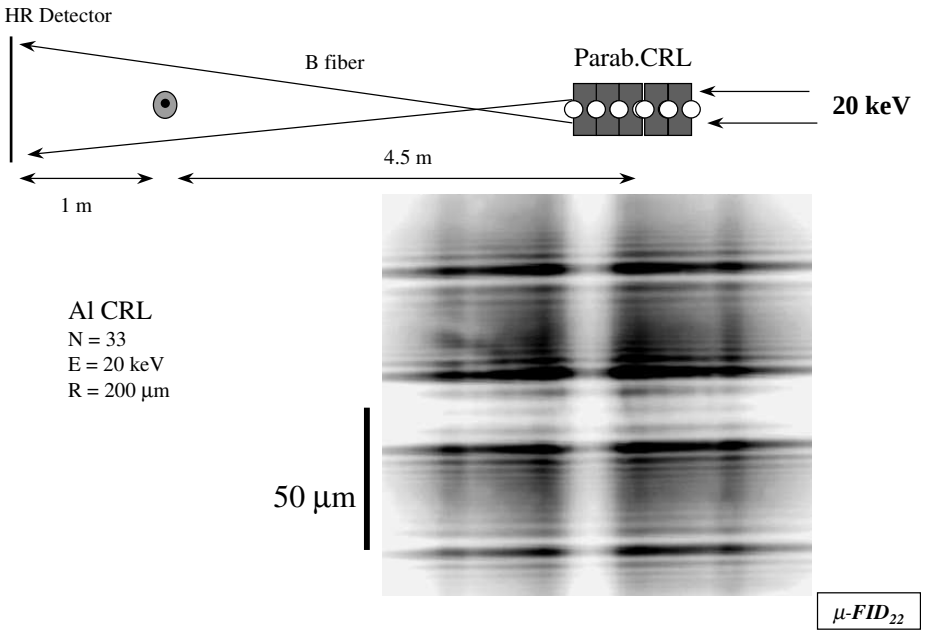

Multilayer

Peter Høghoj, ILL
W/Si: 100 x 22Å (2d)

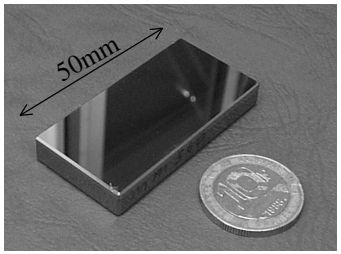

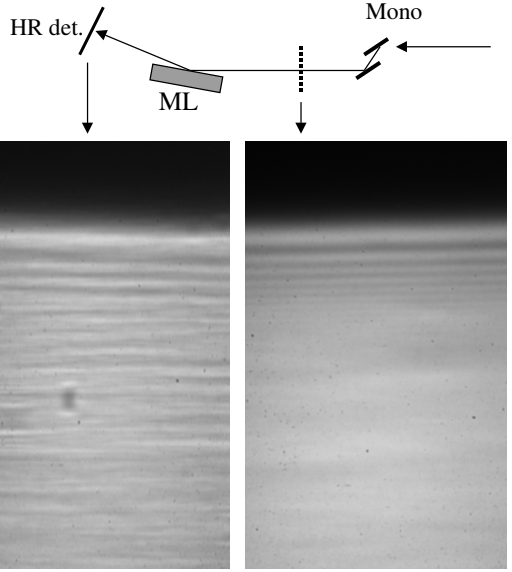

Reflectivity:

E (keV)	%
8	60
14	50
20	65
26	80

Multilayer

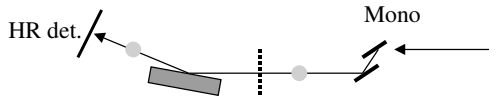

ML

Mono

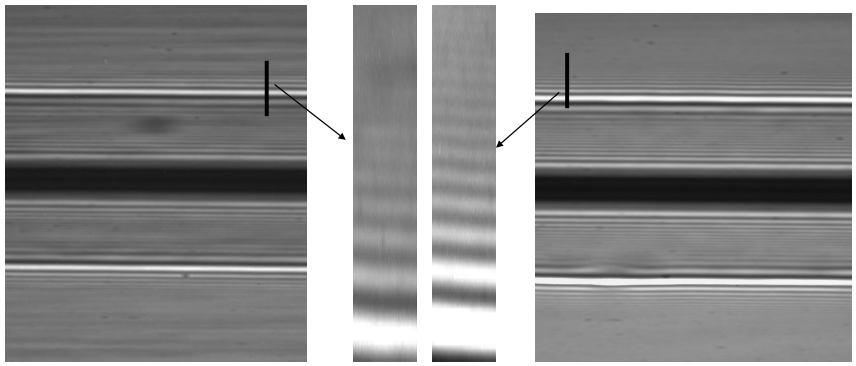

Source size incr. 46% Coherence decr. 32%

Coherence degradation by single assymetrically cut crystals

Case of |b|<1

Asymmetry factor:
$$b = \frac{\sin\theta_0}{\sin\theta_h}$$

Angular aperture:
$$\omega_h = b\omega_0 = \frac{\omega_s}{\sqrt{b}}$$

Spatial aperture:
$$\sigma_h = \frac{\sigma_0}{b}$$

Virtual source:

distance $L_0' = \frac{L_0}{b^2}$

angular aperture

$$\frac{S'}{L_0'} = b\frac{S}{L_0}$$

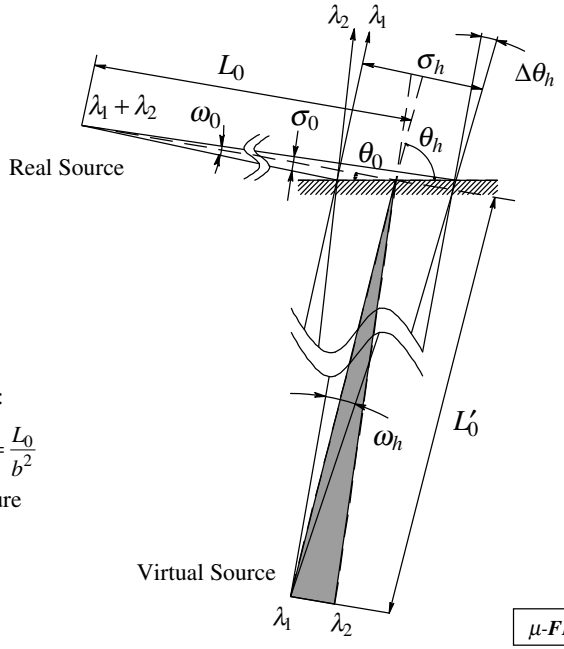

Si (111), E=10 keV, B-fiber at 0.4 m

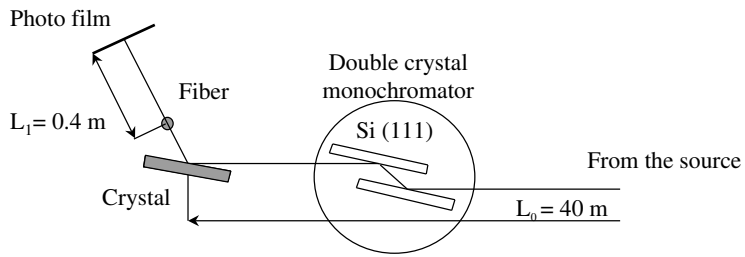

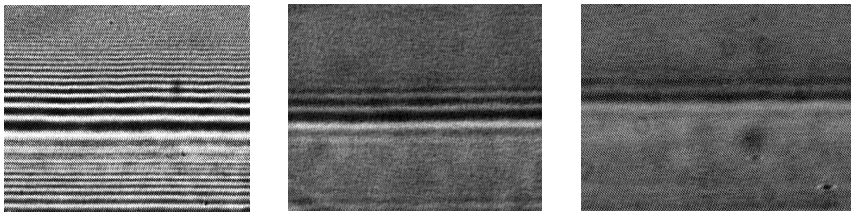

After monochromator Asymmetry factor b = 0.44 Asymmetry factor b = 0.12

Requirements on quality of monochromators

I. Tolerance on miscut for symmetrical reflection

$$|\Delta\varphi| \le \eta \frac{\omega_s}{2\omega_c} \tan\theta_B$$

It can be shown that the allowable miscut does not depend on the wavelength and can be evaluated as

where $\omega_s = S/L_0$ - is source angular aperture
ω_c - is crystal angular aperture
η - is a factor which defines maximum deviation as a fraction of source size

Example:

At energy E=12.4 keV, λ=1 A, Si (111) has
$\theta_B = 9.18^o$, $\omega_c = 4.4''$
Let the source size to be S=40 μm
Let the distance to be L_0=40 m and η=0.1

Then

$|\delta\varphi| < 3.8\ 10^{-4}$ rad (which is ~1')

II. Tolerance on miscut in (+,-) asymmetrical reflection

$$|\Delta\varphi| = \frac{\eta\omega_s \sin^2(\theta_B - \varphi)}{\sqrt{b_1}\omega_c \sin 2\theta_B}$$

Example:

The same parameters as before, plus
$\varphi = 8.48^o$ which gives $b_1 = 4\cdot10^{-2}$, $b_2 = 25$
Then

$|\Delta\varphi| < 10^{-5}$ rad (which is ~2'')

III. Tolerance on temperature difference in (+,-) asymmetrical reflection

$$|\Delta T| \le \frac{\eta\omega_s \sin^2(\theta_B - \varphi)}{\alpha_T \sqrt{b_1}\omega_c \sin 2\varphi \tan\theta_B}$$

Example:

The same parameters as before, plus
$\alpha_T = 2.5\cdot10^{-6}$ K^{-1}
Then

$|\Delta T| < 30^o$

Optics for coherent radiation

- Diffractive optics
  - ***Fresnel Zone Plates***
    - high resolution 0.1 μm at present 50nm in future
      drawbacks: 2-5 μm of metal (Au, Ni etc.) - speckle!
      heatload and radiation damage
  - ***Bragg-Fresnel Optics***
    - resolution 0.2μm - 50nm
    - coherence preservation:
      perfect single crystal + reflection+monochromator
    - high mechanical and temperature stability
      drawback: too narrow bandpass
  - ***Single crystals*** - Bragg (symmetric!) geometry
    - no Laue and asymmetric diffraction!
- Refractive optics
  - cylindrical and parabollic (Al, Be, C …)
    - resolution 0.1 μm 50 nm with parab. Be lenses
- Mirrors, multilayers ?
- Filters - single crystals (Si, diamond etc.)

XFEL Imaging

- Full-field microscopy with incoherent illumination

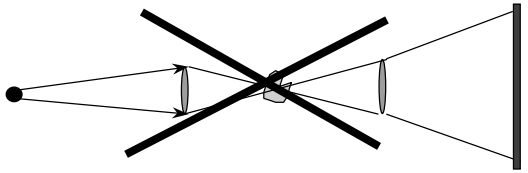

- Full-field microscopy with coherent illumination

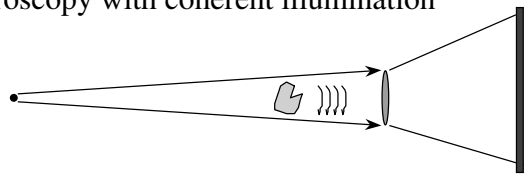

!

- Scanning microscopy

?

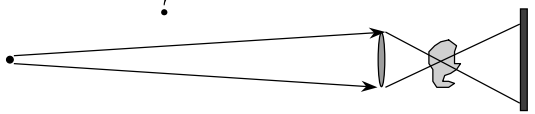

Coherent imaging with XFEL ?

- Resolution
  - full-field imaging < *50 -100 nm*
  - scanning microscopy < *50 nm*
- Fast microtomography - 1mm^3 with *100nm*
  with beam expander - 1cm^3
- Flash imaging
  - phase contrast microscopy
  - diffraction microscopy
  - holographic topography

- *single grains*
- *single cells*
- *HP cells*
- *cracks propagation*
- *crystal growth*
- *HR non perfect crystals*

Conclusion

The first experiments with XFEL will very quickly develop new classes of experiments as they gain experience with their unique source properties